Heliyon 9 (2023) e12576

Contents lists available at ScienceDirect

Heliyon

journal homepage: www.cell.com/heliyon

Research article

Synthesis of nickel nanowires (Ni-NWs) as high ferromagnetic material by electrodeposition technique

Aamir Shahzad [a,*], Ijaz Ahmad Khan [a], Alina Manzoor [a], Muhammad Kashif [a], Muhammad Ahsan [a], Maogang He [b], Jamoliddin Razzokov [c]

[a] Department of Physics, Government College University Faisalabad (GCUF), Allama Iqbal Road, Faisalabad 38040, Pakistan
[b] Key Laboratory of Thermo-Fluid Science and Engineering, Ministry of Education (MOE), Xi'an Jiaotong University, Xi'an 710049, P. R. China
[c] Institute of Fundamental and Applied Research, National Research University TIIAME, Kori Niyoziy 39, 100000 Tashkent, Uzbekistan

ARTICLE INFO

Keywords:
Magnetic nanowires
Nickel anodic aluminium oxide
Electrodeposition
Media storage devices

ABSTRACT

Metallic nanowires (NWs) and their different compounds display incredible prospects for their use in various applications including media storage, sensor and solar cell devices along with the biological drug delivery systems. In this research work, the metallic NWs like nickel nanowires (Ni-NWs) are synthesized successfully by employing electrodeposition process. Anodic aluminum oxide (AAO) templates are employed as a platform with copper metal coating which acts as an active cathode. The synthesized Ni-NWs are examined through various characterization techniques including X-ray diffraction (XRD), scanning electron microscope (SEM) and vibrating sample magnetometer (VSM) to study the crystal structure, surface morphology and magnetic properties, respectively. The XRD analysis shows the development of various diffraction planes like Ni (111), Ni (200), Ni (220) which confirms the formation of polycrystalline nickel NWs. The SEM analysis reveals that the range of diameter and length of nickel NWs are found to be ~160 to 200 and ~4 to 11 micron respectively showing high aspect ratio (ranged from ~200 to 300). The ferromagnetic behavior of Ni-NWs is confirmed by the hysteresis loop carried out for parallel and perpendicular configurations having H_c = 100 and 206 Oe, respectively. The obtained results suggest that the synthesized Ni- NWs may be used for high-density media storage devices.

1. Introduction

In this era of nanotechnology, the nanowires (NWs) and their nanostructured compounds (NSC) have attained enormous attraction because of their distinctive physical and chemical properties. Nanowires with unique nanostructures are studied as one of the promising alternative electrode materials for next generation electrochemical energy devices [1, 2, 3]. The chemical and physical properties of NWs have frequently dominated by their structural behavior like crystallite size and lattice parameters etc and surface morphology like grain size, shape, and distribution of nanoparticles [4, 5, 6]. The enormous growth in the field of information technology (IT) requires processing of massive amount of digital information. The magnetic information carriers require magnetic flux density, large coercivity and acceptable magnetic characterization of synthesized materials which can only be obtained by high-density magnetic nanostructure [7, 8, 9, 10, 11].

The NWs of magnetic materials like nickel, iron, and cobalt have been widely studied because of their incredible applications in the

* Corresponding author.
E-mail addresses: aamirshahzad_8@hotmail.com, aamir.awan@gcuf.edu.pk (A. Shahzad).

https://doi.org/10.1016/j.heliyon.2022.e12576
Received 16 August 2022; Received in revised form 14 November 2022; Accepted 15 December 2022
Available online 23 December 2022

field of electronics, sensors, high-density media storage devices and drug delivery system [12, 13, 14, 15, 16, 17]. Among the ferromagnetic nanostructures, nickel (Ni) has become the prominent candidate for soft sensor applications due to less oxidation problems as compared to their ferromagnetic counterparts. The Ni-NWs surface morphology exhibited high magnetic anisotropy besides exchange interaction which makes it suitable candidate for its use in high-density magnetic media storage applications [18]. The most important factor in the fabrication of NWs is the controlled composition and structural mechanism. Ni-NWs are being synthesized through both physical and chemical vapor deposition methods. However, the electrodeposition method has an edge over formal said methods because of its low manufacturing cost and the ability to produce highly purified products on commercial scale. This template-assisted method is one of the simplest and most frequently used deposition methods to fabricate the anodized aluminum oxide (AAO) di-block co-polymer [19, 20, 21].

Various studies have been performed to investigate and enhance the magnetic character of Ni-NWs. Labchir et al. [22] have examined the influence of an applied magnetic field B (AMF B) on the physical and chemical properties of electrodeposited nickel and cobalt NWS into AAO membranes. It was concluded that the magneto-electrodeposition method offers the possibility of growing and controlling the magnetic properties of one-dimensional (1D) structures. Vorobjova et al. [23] have studied the effect of synthesis conditions of Ni-NWs and porous alumina membrane on the magnetic properties of Ni-NWs arrays. Authors have observed high value of squareness ratio (0.65) and coercivity (750 kOe) under the proposed optimal synthesis conditions for Ni-NW. Tishkevich et al. [24] have formed porous alumina membranes having dimensions (thickness = 50 micron, length = 70 mm and width = 70 mm) to deposit Ni- NWs by electrochemical processing and determined the thermal stability of Ni-NWs into porous alumina template and whole composite.

The AAO template is one of the widely used templates for the deposition of metal NWs because it has an advantage to exactly control the diameter of NWs which has been confirmed by the pore size of templates [25, 26, 27].

2. Experimental setup

For this research work, the AAO templates were commercially purchased from Whatman, USA. The electron beam (e-beam) physical vapor deposition method was used to coat a thin layer of copper (Cu) (thickness = ~220 nm) to one side of AAO templates. This coated side of AAO template acts like a cathode as shown in Figures 1 and 2. One molar solution of an electrolyte was prepared from nickel sulphate hexahydrate by mixing it into deionized water. The pH was adjusted to 3 by using 0.1 M sulfuric acid and buffered

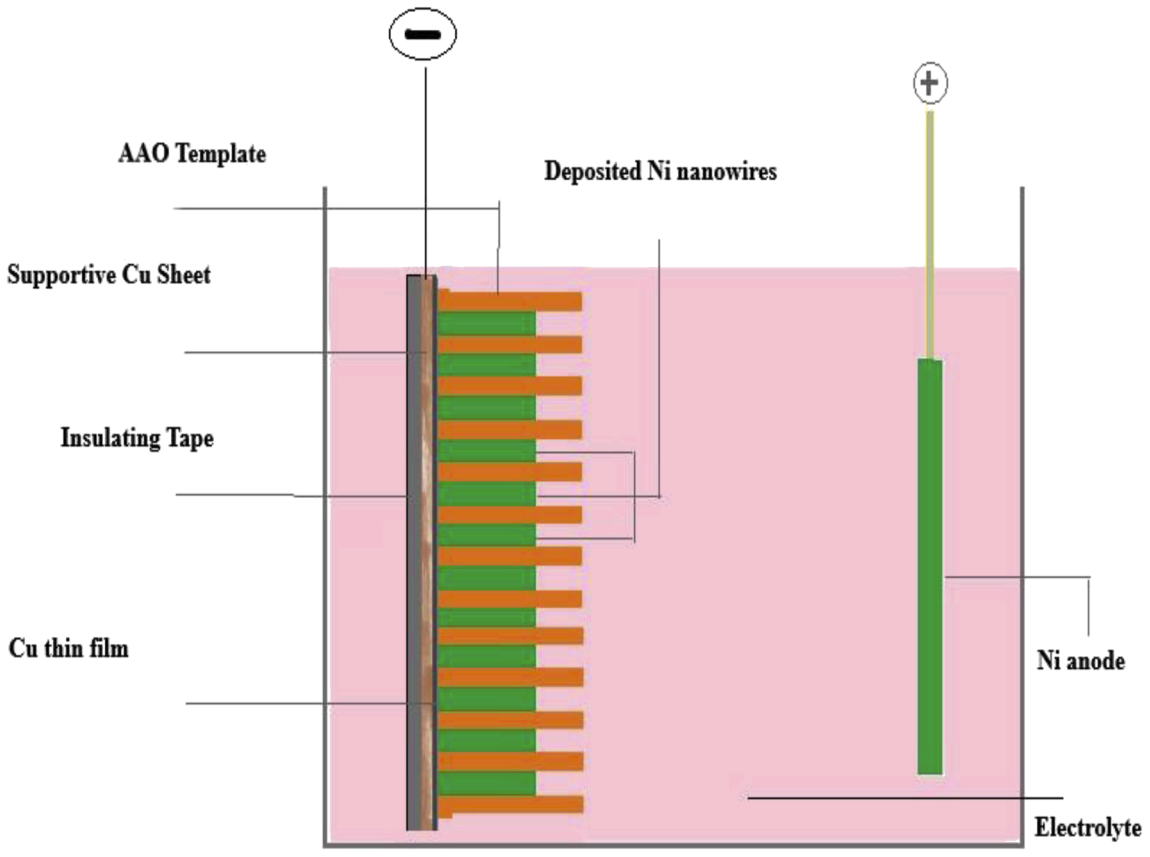

Figure 1. Simplified diagram of electrodeposition for Nickel Nanowires.

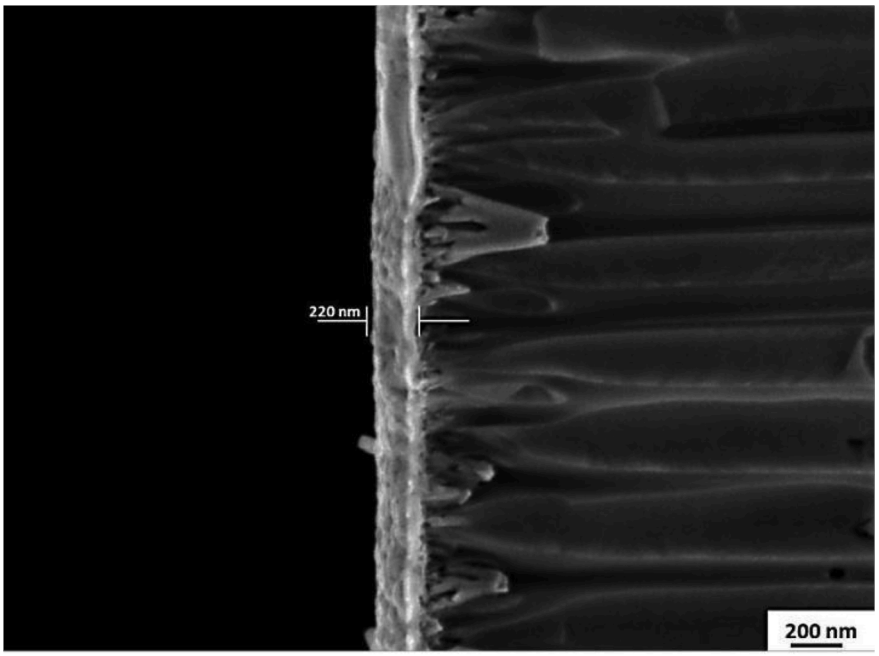

Figure 2. Thickness of Copper layer on the backside of template (220 nm).

by 0.2 M boric acid for longer plating life. In our case, it was taken fixed 120 min deposition time to complete fill out the pores at template. The deposition potential and current density were adjusted to 2.1 V and 1.5 mA/cm^2, respectively. The schematic diagram illustrating the synthesis process of NWs is shown in Figure 1. The pure nickel wire (thickness = 1 mm) indicated by the positive sign will act as an anode while the Cu layer coated by e-beam deposition technique will act as cathode. However, a pure Cu sheet (thickness = 1 mm) is attached to the backside of thin conducting layer to provide support and electric current. The backside of Cu sheet is protected from deposition using adhesive insulation tape. When the deposition process starts, the Ni^{+2} is reduced to nickel and deposited into the pores of templates and the development of pure 1D Ni-NWs started as shown by the green color in Figure 1.

The synthesized Ni-NWs were investigated by X-ray diffraction (XRD), scanning electron microscope (SEM) and vibrating sample magnetometer (VSM) in order to study the crystal structure, crystalline nature, surface morphology (NWs) and magnetic properties like hysteresis loop. To study the morphology of NWs, the template is allowed to dissolve into 2 M aqueous solution of NaOH. To collect well-aligned Ni-NWs and after that it washed several times with deionized water for investigating the other physical properties.

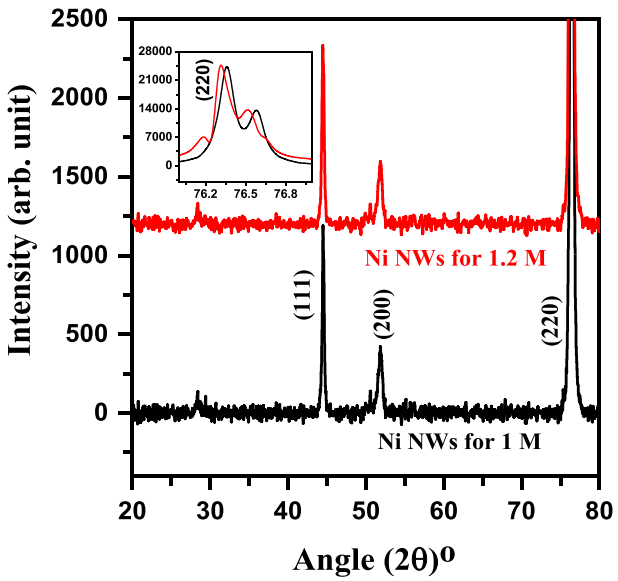

Figure 3. XRD pattern for Ni NW's with different [1M (black) and 1.2 M (red)] concentrations.

3. Results and discussion

In this section, we analyze crystal structure behaviors of NWs in template and Ni-NWs with AAO by XRD (D8 Advance, Bruker, USA). The surface morphology of Ni- NWs with different concentrations of nickel sulphate hexahydrate was investigated by SEM (JSM-6490A, JEOL Japan). The magnetic properties of Ni-NWs with parallel and perpendicular configurations were studied by VSM (VSM-175, YP magnetic technology development, China).

3.1. Structural analysis

The XRD patterns reveal the structural changes in all synthesized samples when the NWs are still in the template and the Ni-NWs are embedded into AAO. Figure 3 (marked black) demonstrates the structural changes in sample-1 (1M solution of nickel sulphate hexahydrate) having controlled pH and potential of the order of 2.1V. For 1M solution of nickel sulphate hexahydrate, the development of Ni (220) plane shows that the nickel NWs are grown along (220) orientation. The development of Ni (111), Ni (200) and Ni (220) diffraction planes confirms the polycrystalline nature of nickel NWs having FCC crystal structure [18]. The intensities of Ni (111) and Ni (200) diffraction planes appeared at 2θ values of 44.51° and 51.84° are significantly smaller as compared to Ni (220) planes which show that the Ni-NWs grow preferably along (220) orientation. The appearance of shoulder peak along Ni (220) plane indicates the presence of defects and micro strains developed in the synthesized Ni-NWs during the synthesis process.

The structural parameters like lattice constant "a", crystalline size "D", and X-ray density "$d_{x\text{-}ray}$" are determined by using the following relations.

$$a = \frac{\lambda}{2\,Sin\,\theta}\sqrt{h^2 + k^2 + l^2} \tag{1}$$

$$D = \frac{k\lambda}{\beta_{hkl}\,Cos\,\theta} \tag{2}$$

$$d_{x-ray} = \frac{ZM}{N_A V} \tag{3}$$

where, in above Eqs. (1), (2), and (3), λ, k, β, θ, Z, M, N_A and V are the wavelength of X-ray source, numerical constant, full-width half maxima (FWHM) of any diffraction plane, Braggs angle, number of atoms in unit cell, molecular weight, Avogadro number and unit cell volume.

It is found that the average value of D (Eq. (2)) for sample-1 is ~21.60 nm. The value of D has increased with increasing the deposition rate, which strongly effect the crystallite size [24]. It worth noticing that the deposition rate is also associated with the increase of substrate surface transient temperature which affects the D values of synthesized films like Zirconia and ZrON. Different research groups have also reported that the structural parameters like micro-strains, stresses and defects are affected by the increase of substrate surface transient temperature [28, 29, 30]. Moreover, Labchir et al. [31] have studied the Co and Ni nanowires synthesized by magneto-electrodeposition process and discussed their structural parameters. The value of "a" for Ni (220) plane is found to be 3.514 Å which is well matched with the standard value (JCPDS: 00-04-0850) for nickel.

Figure 3 (marked red) shows the XRD pattern of Ni-NWs synthesized with 1.2M solution of nickel sulphate hexahydrate (sample-2). The development of Ni (111), Ni (200) and Ni (220) diffraction planes again confirm the formation of crystalline nature of Ni- NWs having no traces of Al_2O_3 phase because no diffraction plane related to Al_2O_3 phase is observed. Moreover, the intensity of Ni (220)

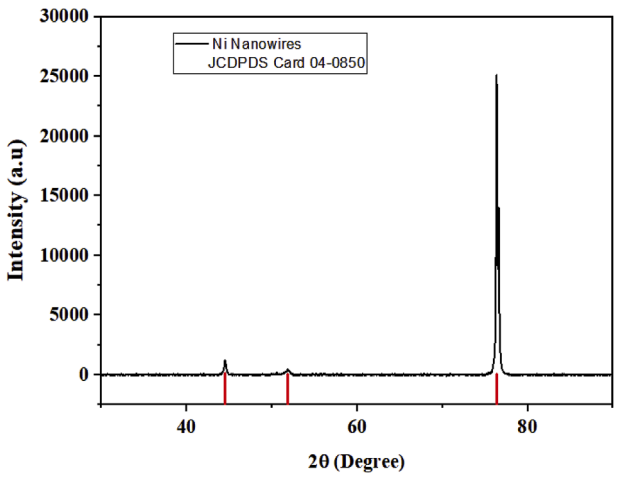

Figure 4. XRD of embedded Nickel Nanowire and Standard JCPDS card 00-04-0850 of FCC Nickel.

plane is showing that the synthesized Ni-NWs are grown preferentially along (220) orientation. It is concluded that there is a slight increase in peak intensity with increasing M of nickel sulphate hexahydrate is observed.

The average values of *D* for nickel NWs synthesized for 1.2 M solution of nickel sulphate hexahydrate is found to be ~20.38 nm. The value of "*a*" for (220) plane is equal to 3.495 Å. XRD results shows that the average values of "*D*" and "*a*" are decreased with the increasing M of nickel sulphate hexahydrate. The XRD results are well matched with the values reported by Pratama et al. [28]. The development of diffraction planes related to Ni phase is in good agreement with the standard data (see Figure 4). The observed values of d-spacing for all diffraction planes related to Ni phases are slightly higher than standard values (Table 1). Thus it can be concluded that the lattice constant of all diffraction planes related to Ni Phases have been increased with increasing concentration of nickel sulphate hexahydrate.

3.2. Microstructural analysis

The surface morphology of nickel NWs synthesized for various M solution of nickel sulphate hexahydrate is investigated by employing SEM analysis. Four panels of Figure 5(a–d) display the descriptive microstructures of nickel NWs synthesized for 1 M solution of nickel sulphate hexahydrate taken at various magnifications (×2000, ×5000, ×10,000, ×30,000). The SEM microstructures reveal the formation of NWs which are distributed uniformly but making complicated network of NWs. The uniform but complicated distribution of NWs indicate the presence of empty region, however the empty region is smaller than the covered. The length of Ni- NWs is ranged from ~3 to ~8 micron while the diameter of NWs is in the range of ~111 to 222 nm, respectively. The development of parallel, perpendicular and inclined configurations of NWs makes a complex network. The clear visualization of surface morphology of Ni-NWs and their distribution can be viewed from magnified SEM microstructures (see Figures 5 and 6). The formation of nickel NWs results in better conductance if used as transparent electrodes. Different panels of Figure 6(a–d) demonstrate the descriptive microstructures of Ni-NWs synthesized for 1.2 M solution of nickel sulphate hexahydrate taken at various magnifications (×2500, ×5000, ×10,000, ×20,000). The distribution of nickel NWs is homogeneous having an average length of ~few micron and diameter of ~0.5 micron. The length of Ni-NWs is ranged from ~4 to 11 micron while the diameter of NWs is ranged from ~160 to 200 nm, respectively It is obvious from the SEM microstructures that the grown Ni- NWs posses high packing density. It is known that the electrodeposition is a bottom-up approach and the synthesized Ni-NWs on copper cathode seems to grow along with the pores towards the top. The SEM microstructure indicates the parallel configuration of NWs and condenses on the template surface making complex microstructure. The SEM analysis indicates that the development of Ni-NWs have several micron lengths which may be due to the quite reasonable pore-filling factor of template.

3.2.1. Pore filling factor and aspect ratio

The total number of nano-pores across the entire template and the average diameter of NW's aspect ratio has been calculated and results are as under: the size of single nano-pore, thickness of pore-wall of nano-pore, total length covered by nano-pore and nano-wall and average diameter of AAO template are about 300, 20, 320 nm and 2.5 cm (25 nm), respectively. The area of a circular disc and surface area required by single nano-pores are found to be 4.9×10^{14} nm^2 and 1.024×10^4 nm^2, therefore, the total number of nano-pores in 490×10^{12} nm^2 area will be 4.875×10^{10} nano-pores. Practically, the number of Ni-NWs is less than nano-pores in the template due to 70 % pore filling factor which is because of some blocked and branched pores or have defects during the synthesis process of template. Based on above calculation, for 70 % pore-filling factor, the number of NWs deposited inside the AAO template can be calculated by the following relation.

$$\text{Number of NWs} = (\text{Total No of Nano} - \text{pores}) \times (\text{Pore} - \text{filling Factor})$$

Therefore, the number of NWs deposited inside the AAO template having diameter (25 mm) and pore size (100 nm) is found to be 3.349×10^9 NWs. Moreover, the aspect ratio of Ni- NWs can be calculated by the following relation.

$$\text{Aspect ratio} = \frac{\text{Length of NWs}}{\text{Diameter of NWs}}$$

The values of aspect ratio is found to be 160 to 200 while the length and diameter of Ni-NWs are ranged from ~4 to 11 micron and ~160–200 nm, respectively. However, the average diameter of NW's is about 175 nm with a high aspect ratio of 200.

3.3. VSM analysis

The magnetic properties like hysteresis loop of Ni-NWs are carried out for both perpendicular and parallel configurations for the sample synthesized in 1 M solution of nickel sulphate hexahydrate. These measurements are carried out by still embedded the NWs into

Table 1
Comparison of experimental and standard values of diffraction angle and d-spacing.

Sr. No	hkl	Angle (2θ)° [Observed]	d-spacing (Å) [Observed]	Angle (2θ)° [Standard]	d-spacing (Å) [Standard]
1	(111)	44.42	2.03781	44.508	2.03400
2	(200)	51.80	1.76350	51.847	1.76200
3	(220)	76.33	1.24658	76.372	1.24600

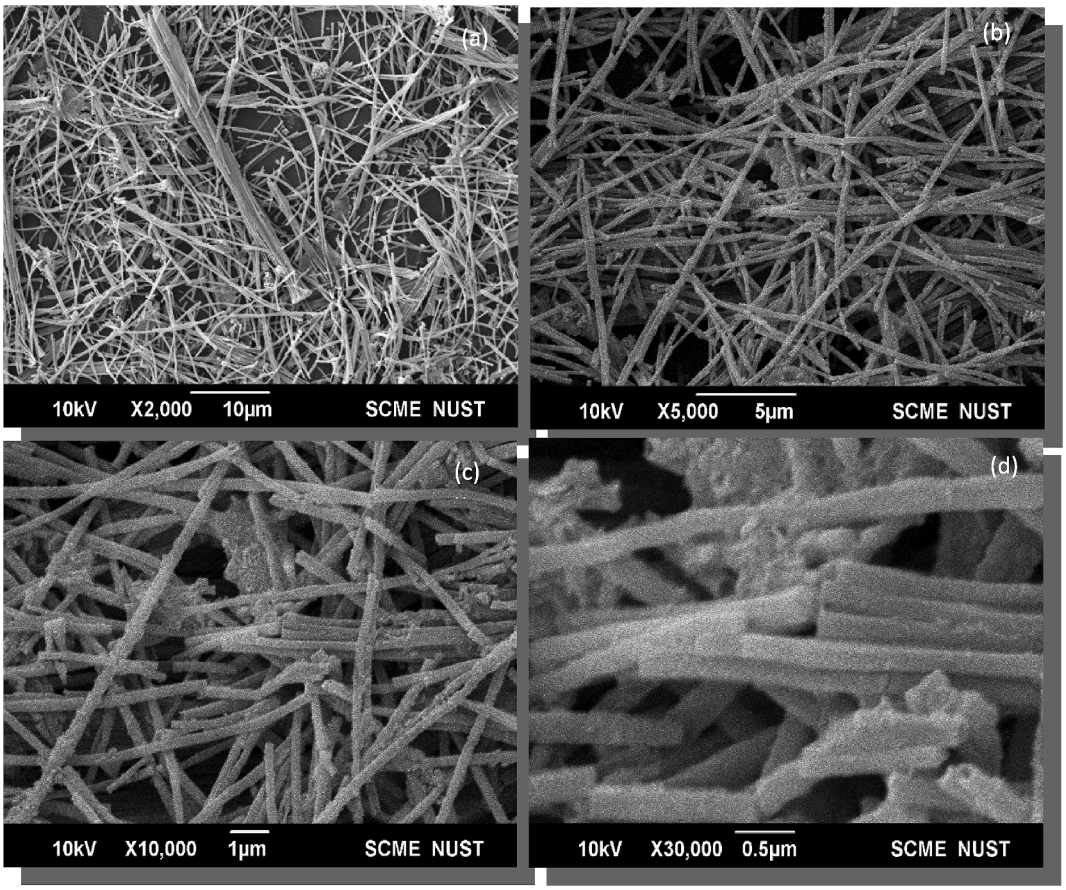

Figure 5. SEM micrograps of electrodeposited Ni NW's (sample 1) and at various magnifications (a) ×2000, (b) ×5000, (c) ×10,000 and (d) ×30,000.

AAO template.

3.3.1. MH loop for parallel configuration

Figure 7 demonstrates the hysteresis loop of Ni-NWs synthesized (still embedded in AAO templates) for 1 M solution of nickel sulphate hexahydrate. The static magnetic analysis for parallel configuration (applied magnetic field parallel to the length of NW's) is carried out at room-temperature under 5 T magnetic fields. The shape of hysteresis loop confirmed the ferromagnetic behavior of Ni-NWs. It is observed from the MH curve that the values of coercivity (Hc), retentivity (Mr), saturation magnetization (Ms) and squareness (Mr/Ms) for parallel configuration are found to be ~100 Oe, ~1.13 emu/g, 18 emu/g and 0.06, respectively. The insets of Figure 7 show the hysteresis curve of Ni- NWs at low magnetic fields (about origin).

3.3.2. MH loop for perpendicular configuration

Figure 8 shows the hysteresis loop of Ni- NWs synthesized for 1M solution of nickel sulphate hexahydrate embedded in AAO template for perpendicular configuration (applied magnetic field perpendicular to the length of NW's). The value of Hc is found to be ~206 Oe which is almost two times higher than that for parallel configuration as well as sufficiently greater than the reported values [18]. The value of Mr is found to be 3.63 emu/g that is 3.2 times higher as compared to measured value of Mr for parallel configuration. It is interesting to note that the value of Ms is approximately the same but the value of Mr/Ms is found to be 0.2 times of parallel configuration value. The values of above parameters are in good agreement with the reported values [28]. It is also known that the value of Hc for Ni- NWs is greater than bulk nickel [32]. Results indicate that the value of Hc for ~11 micron long Ni-NWs is found to be ~206 Oe which is 5.15 times than bulk nickel having grain size (~10 micron). This indicates that nickel NWs have harder ferromagnetic behavior as compared to bulk nickel which is due to anisotropy in the shape, size, and distribution of nickel Ni-NWs [33]. The higher aspect ratio of NWs may be the other reason. The insets of Figures 7 and 8 show the hysteresis loop about origin for NWs synthesized for parallel and perpendicular configurations. Figure 9 shows the real time comparison of hysteresis loops when magnetic field is applied to the length of Ni-NWs with parallel and perpendicular configurations while inset of Figure 9 represents the values of squareness observed for Ni-NWs having perpendicular configurations. TableII demonstrates that the values of squareness for perpendicular configuration are higher than for parallel configuration of Ni- NWs. This shows that an easy magnetization is developed

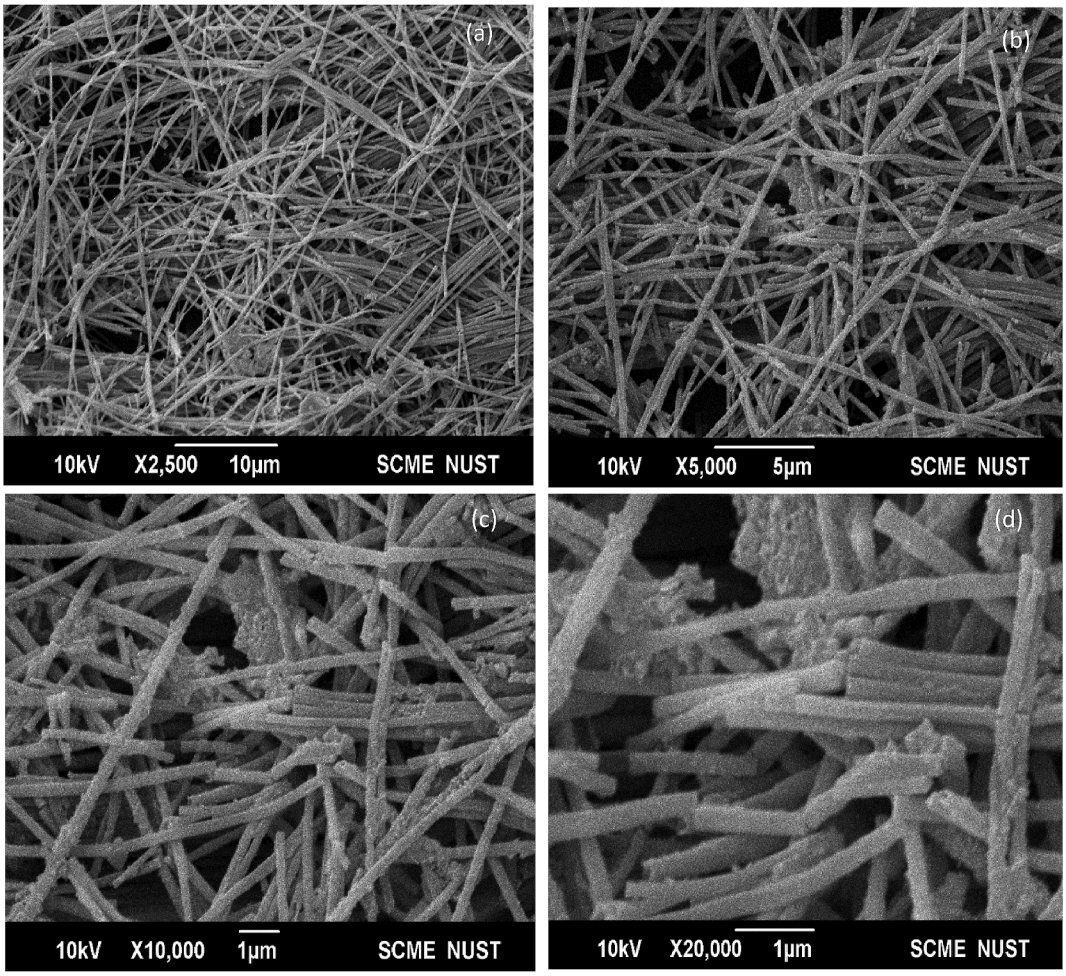

Figure 6. SEM micrographs of electrodeposited Ni NW's (sample 2) and at various magnifications (a) ×2000, (b) ×5000, (c) ×10,000 and (d) ×30,000.

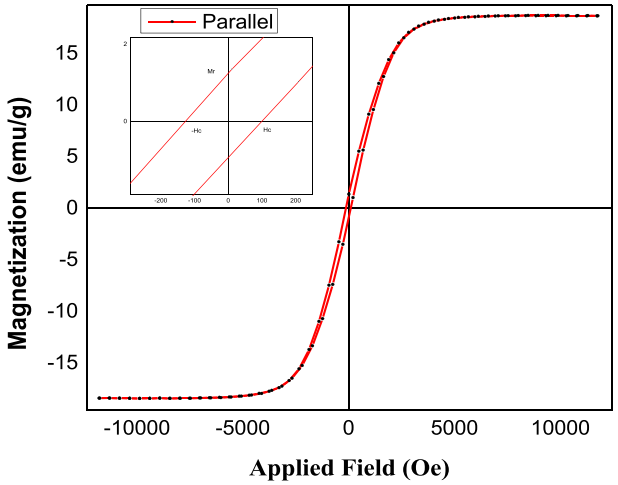

Figure 7. Hysteresis Loop of Nickel Nanowires with parallel configuration.

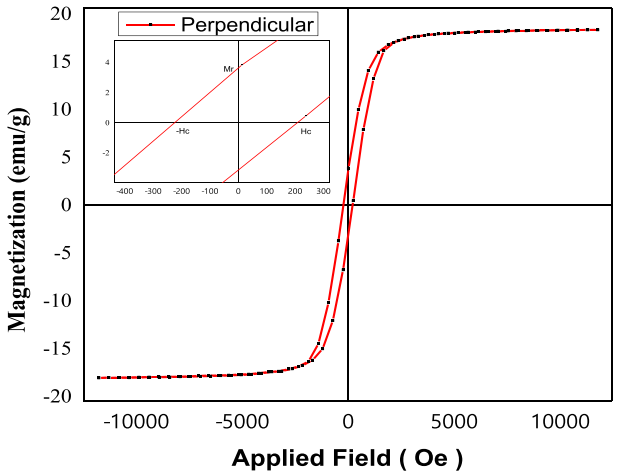

Figure 8. Hysteresis Loop of Nickel Nanowires with perpendicular configuration.

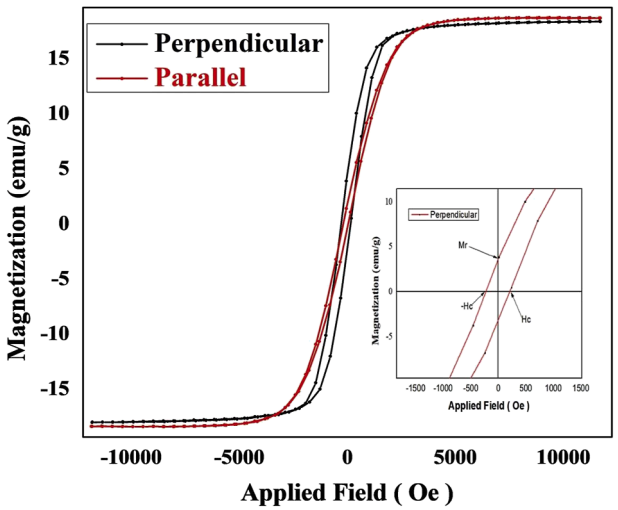

Figure 9. M–H curve for parallel and perpendicular configuration to the length of Nickel nanowires (b) Inset is out of plane squareness of Ni NW's.

in the perpendicular direction to the length of Ni-NWs. This magnetic behavior of Ni- NWs and their strong ferromagnetic nature makes it possible to use them for magnetic media recording and storage devices.

4. Conclusions

Template-assisted Ni-NWs have been successfully synthesized using electrodeposition technique. The development of various diffraction planes confirmed the formation of polycrystalline nickel NWs. Polycrystalline Ni-NWs with FCC structure revealed a reasonable pore-filling factor (70 %). The SEM microstructures uncovered that the Ni-NWs are independent, well-aligned, and parallel to each other with a high aspect ratio of ~300 nm. The coercivity for perpendicular configuration of Ni-NWs is found to be greater (206 Oe) than that of parallel configuration (100 Oe). The value of H_c (~206 Oe) for ~11-micron long Ni- NWs is found to be 5 times greater than bulk nickel having grain size (~10 micron), indicating harder ferromagnetic behavior of Ni-NWs as compared to bulk nickel. The magnetic behavior of polycrystalline Ni- NWs is found to be enhanced as compared to bulk nickel of the same size, revealing the strong ferromagnetic nature of Ni-NWs. Investigated magnetic behavior of Ni-NWs and their strong ferromagnetic nature makes it possible to use them for magnetic media recording and storage devices.

Table 2
Comparison of magnetic parameters for both parallel and perpendicular configurations.

Parameters	Parallel configuration	Perpendicular configuration
Coercivity (Hc)	100 Oe	206 Oe
Retentivity (Mr)	1.13 emu/g	3.63 emu/g
Saturation magnetization (Ms)	18 emu/g	18 emu/g
Squareness (Mr/Ms)	0.06	0.20

Declarations

Author contribution statement

Aamir Shahzad: Conceived and designed the experiments; Analyzed and interpreted the data; Wrote the paper.
Ijaz Ahmad Khan: Wrote the paper; Analyzed and interpreted the data.
Alina Manzoor: Wrote the paper; Analyzed and interpreted the data.
Muhammad Kashif: Analyzed and interpreted the data; Contributed reagents, materials, analysis tools or data.
Muhammad Ahsan: Performed the experiments; Contributed reagents, materials, analysis tools or data; Wrote the paper.
Maogang He: Wrote the paper, Analyzed and interpreted the data.
Jamoliddin Razzokov: Analyzed and interpreted the data, Wrote the paper.

Funding statement

This research did not receive any specific grant from funding agencies in the public, commercial, or not-for-profit sectors.

Data availability statement

Data will be made available on request.

Declaration of interests statement

The authors declare no conflict of interest.

Additional information

No additional information is available for this paper.

Acknowledgements

The authors thank Khurram Shahzad (Project Director), TEVTA-MIDC, Sialkot, for providing facilities to test and run our Experiment. This work was partially supported by the industrial collaborative work between Government College University Faisalabad (GCUF) and Metal Industries Development Complex (MIDC) Sialkot, TEVTA, Govt. of Punjab, Pakistan, as a position of Consultant in a proposed project.

References

[1] Adrià Garcia, Subhajit Biswas, David McNulty, Ahin Roy, Sreyan Raha, Sigita Trabesinger, Valeria Nicolosi, Achintya Singha, Justin D. Holmes, ACS Appl. Energy Mater. 5 (2022) 1922–1932.
[2] Tomasz Wasiak, Dawid Janas, J. Alloys Compd. 892 (2022), 162158.
[3] Martha Claros, Jan Kuta, Omar El-Dahshan, Jan Michalička, Yecid P. Jimenez, Stella Vallejos, J. Mol. Liq. 325 (2021), 115203.
[4] Xinghua Meng, Da Deng, Chem. Eng. Sci. 194 (2019) 134–141.
[5] O.M. Zhigalina, I.M. Doludenko, D.N. Khmelenin, D.L. Zagorskiy, S.A. Bedin, I.M. Ivanov, Crystallography 63 (2018) 480–484.
[6] A. Manzoor, M.A. Khan, Amir Muhammad Afzal, Muhammad Imran Arshad, A. Shahzad, S. Tahir, M. Kashif, G. Abbas Ashraf, M.Y. Khan, M.N. Rasul, M.S. Shifa, G. Nasar, A. Hussain, Ceram. Int. 48 (2022) 32266–32272.
[7] Mariana P. Proenca, Nanomaterials 12 (2022) 1308.
[8] M. Nastasi, D.M. Parkin, H. Gleiter, Mechanical Properties and Deformation Behavior of Materials Having Ultra-fine Microstructures 233, Springer Science & Business Media, 2012.
[9] A. Samardak, E. Sukovatitsina, A. Ognev, L. Chebotkevich, R. Mahmoodi, S. Peighambari, M. Hosseini, F. Nasirpouri, J. Phys.: Conf. Ser. (2012), 012011.
[10] J. Spiegel, I. Huynen, Solid State Phenom. 152–153 (2009) 389–393.
[11] Pascal Scholzen, Guillaume Lang, Andrey S. Andreev, Alberto Quintana, James Malloy, Christopher J. Jensen, Kai Liu, Jean-baptiste d'Espinose de Lacaillerie, Phys. Chem. Chem. Phys. 24 (2022) 11898–11909.
[12] Claudia Fernández-González, Alejandra Guedeja-Marrón, Beatriz L. Rodilla, Ana Arché-Nuñez, Rubén Corcuera, Irene Lucas, María Teresa González, Maria Varela, Patricia de la Presa, Lucía Aballe, Lucas Pérez, Sandra Ruiz-Gómez, Nanomaterials 12 (2022) 2565.
[13] Joseph Um, Yali Zhang, Zhou Wen, R. Mohammad, Kouhpanji Zamani, Cosmin Radu, Rhonda R. Franklin, J. Bethanie, H. Stadler, ACS Appl. Nano Mater. 4 (2021) 3557–3564.
[14] Giuseppe Muscas, Petra E. Jönsson, I.G. Serrano, Örjan Vallin, M. Venkata Kamalakar, Nanoscale 13 (2021) 6043.

[15] O. Kazakova, J. Gallop, P. See, D. Cox, G. Perkins, J. Moore, L. Cohen, IEEE Trans. Magn. 45 (2009) 4499–4502.
[16] A. Manzoor, M.A. Khana, A. Shahzad, T.I. Al-Muhimeed, A.A. AlObaid, H. Albalawid, A.M. Afzale, M. Kashifb, S. Tahirb, T. Munir, Ceram. Int. 47 (2021) 22662–22668.
[17] Evgeny Katz, Magnetochemistry 5 (2019) 61.
[18] M.M. Imran, J. Alloys Compd. 455 (2008) 17–20.
[19] A. Huczko, Appl. Phys. A 70 (2000) 365–376.
[20] L. Wen, R. Xu, Y. Mi, et al., Nat. Nanotechnol. 12 (2017) 244–250.
[21] E. Davoodi, M. Zhianmanesh, H. Montazerian, et al., J. Mater. Sci. Mater. Med. 31 (2020) 60.
[22] N. Labchir, A. Hannour, D. Vincent, A. Ihlal, M. Sajieddine, Curr. Appl. Phys. 25 (2021) 33–40.
[23] A. Vorobjova, et al., RSC Adv. 11 (2021) 3952–3962.
[24] D. Tishkevich, A. Vorobjova, A. Trukhanov, Solid State Phenom. 299 (2020) 281–286.
[25] L. Cagnon, Y. Dahmane, J. Voiron, S. Pairis, M. Bacia, L. Ortega, N. Benbrahim, A. Kadri, J. Magn. Magn Mater. 310 (2007) 2428.
[26] Mozalev Alexander, Jaromir Hubalek, Electrochim. Acta 297 (2019) 988–999.
[27] M.R. Koblischka, A. Koblischka-Veneva, Fabrication of superconducting nanowires using the template method, Nanomaterials 11 (2021) 1970.
[28] S.N. Pratama, Y. Kurniawan, S. Muhammady, K. Takase, Y. Darma, Mater. Res. Express 5 (2018), 034008.
[29] I. Khan, B. Freeha, U. Ikhlaq, R. Rawat, R. Ahmad, J. Fusion Energy 34 (2015) 930–940.
[30] I. Khan, U. Ikhlaq, A. Farid, R. Rawat, R. Ahmad, J. Fusion Energy 34 (2015) 1284–1296.
[31] Nabil Labchir, Abdelkrim Hannour, Abderrahim Ait hssi, Didier Vincent, Ahmed Ihlal, Mohammed Sajieddine, Curr. Appl. Phys. 25 (2021) 33–40.
[32] S. Dwivedi, H.C. Nayak, S.S. Parmar, R.P. Kumhar, S. Rajput, Calcination temperature Reflected structural, optical and magnetic properties of nickel oxide, Magnetism 2 (2022) 45–55.
[33] Fernando Meneses, Silvia E. Urreta, Juan Escrig, Paula G. Bercoff, Curr. Appl. Phys. 18 (2018) 1240–1247.